Geophysical Research Letters

RESEARCH LETTER
10.1029/2022GL098353

Key Points:

- In comparison with Al-free shy-B, the incorporation of 11.7 wt.% Al_2O_3 in superhydrous phase B (shy-B) expands the stability by ~400–800 K at 20–30 GPa
- Al-bearing phase D could be present even at normal mantle geotherm conditions at 30–40 GPa
- δ-AlOOH is the stable hydrous phase coexisting with Al-depleted bridgmanite at pressures above 52 GPa

Supporting Information:

Supporting Information may be found in the online version of this article.

Correspondence to:

X. Li,
lixinyang@jlu.edu.cn

Citation:

Li, X., Speziale, S., Koch-Müller, M., Husband, R. J., & Liermann, H.-P. (2022). Phase stability of Al-bearing dense hydrous magnesium silicates at topmost lower mantle conditions: Implication for water transport in the mantle. *Geophysical Research Letters*, *49*, e2022GL098353. https://doi.org/10.1029/2022GL098353

Received 1 MAR 2022
Accepted 8 AUG 2022

Author Contributions:

Conceptualization: Xinyang Li, Sergio Speziale, Monika Koch-Müller, Hanns-Peter Liermann
Data curation: Xinyang Li
Formal analysis: Xinyang Li
Funding acquisition: Sergio Speziale, Monika Koch-Müller, Hanns-Peter Liermann
Investigation: Xinyang Li, Rachel Jane Husband
Methodology: Xinyang Li

Phase Stability of Al-Bearing Dense Hydrous Magnesium Silicates at Topmost Lower Mantle Conditions: Implication for Water Transport in the Mantle

Xinyang Li[1,2], Sergio Speziale[2], Monika Koch-Müller[2], Rachel Jane Husband[1], and Hanns-Peter Liermann[1]

[1]Deutsches Elektronen-Synchrotron DESY, Hamburg, Germany, [2]GFZ German Research Centre for Geosciences, Potsdam, Germany

Abstract In this study, we investigated the phase stability of Al-free and Al-bearing superhydrous phase B (shy-B) up to 55 GPa and 2500 K. In comparison with Al-free shy-B, the incorporation of 11.7 wt.% Al_2O_3 in shy-B expands the stability by ~400–800 K at 20–30 GPa. The determined dehydration boundary for Al-bearing phase D indicates that it could be present even at normal mantle geotherm conditions at 30–40 GPa. Up to 23.8 mol.% Al_2O_3 can be dissolved into the structures of akimotoite and bridgmanite as a result of the decomposition reactions of Al-bearing shy-B and phase D between 20 and 40 GPa. Results of further experiments indicate that δ-AlOOH is the stable hydrous phase coexisting with Al-depleted bridgmanite at pressures above 52 GPa. This study shows that the incorporation of Al in dense hydrous magnesium silicates can have a profound impact on our picture of the water cycle in the deep Earth.

Plain Language Summary Constraining the deep cycle of water has a tremendous impact on our picture of the current state of the Earth and the evolution of the Earth's interior. Dense hydrous magnesium silicates (DHMSs) are considered potential H_2O carriers in the Earth's mantle. However, the DHMSs can only be present at the relatively cold conditions of subduction slabs due their limited thermal stability. We determined the phase stability of Al-bearing DHMSs at high pressure and temperature (P-T) conditions. Our results show that the thermal stability of Al-bearing shy-B extends by 400–800 K with respect to its Al-free counterpart at 600–800 km depth. The incorporation of Al also expands the phase stability of phase D and enhances the likelihood of its occurrence at normal mantle conditions at 800–1100 km. In addition, we observe that 23.8 mol.% Al_2O_3 can be dissolved into the structures of akimotoite and bridgmanite as a result of the decomposition reactions of Al-bearing shy-B and phase D between 600 and 100 km depth. Furthermore, δ-AlOOH is the stable hydrous phase coexisting with Al-depleted bridgmanite in the MgO-SiO_2-Al_2O_3-H_2O system at pressures above 52 GPa and 1500 K.

1. Introduction

Ice-VII, brucite and hydrous ringwoodite were found in diamond inclusions indicating the occurrence of free H_2O-bearing fluids and hydrous minerals in the transition zone (TZ) and the uppermost lower mantle (ULM) (Palot et al., 2016; Pearson et al., 2014; Tschauner et al., 2018). Seismic low velocity zones (LVZs) observed by seismology in the ULM might be related to the presence of melts associated with dehydration of hydrous minerals (Liu, Irifune, et al., 2016; Schmandt et al., 2014). There are also many high anisotropy regions with large shear wave splitting at the depth of the TZ and ULM near subducted slabs (e.g., Brudzinski & Chen, 2003; Di Leo et al., 2012; Wookey et al., 2002). The seismic anisotropy observed in these regions has been attributed to the presence of dense hydrous magnesium silicates (DHMSs) such as superhydrous phase B (shy-B) and phase D (Ph-D) (Rosa et al., 2013, 2015). DHMSs are potential H_2O carriers into the deep Earth (e.g., Frost, 1999; E. Ohtani, 2005). Thus, investigating their physical properties and phase stabilities is important to understand seismic anomalies in the deep inside of our planet (e.g., Koch-Müller et al., 2005; Li et al., 2016; E. Ohtani, 2020; Yang et al., 2017).

The thermal phase stability field of Mg-endmember shy-B ($Mg_{10}Si_3O_{18}H_4$) in the system MgO-SiO_2-H_2O (MSH) was examined up to 31 GPa and the results indicate that shy-B remains stable up to 23 GPa and 1700 K above which it decomposed to hydrous ringwoodite (Ohtani et al., 2003). At pressures higher than 30 GPa shy-B decomposes to Ph-D, MgO and bridgmanite at 900 K (Ohtani et al., 2003). The phase stability of Mg-endmember Ph-D

Project Administration: Sergio Speziale, Monika Koch-Müller, Hanns-Peter Liermann
Supervision: Sergio Speziale, Monika Koch-Müller, Hanns-Peter Liermann
Writing – original draft: Xinyang Li
Writing – review & editing: Sergio Speziale, Monika Koch-Müller, Rachel Jane Husband, Hanns-Peter Liermann

was examined up to 25 GPa and 1700 K using a large volume press (LVP) and up to 53 GPa at 2100 K in a laser heated diamond anvil cell (Frost & Fei, 1998; Shieh et al., 1998). Al_2O_3 is a major chemical component of the solid Earth, and the Al_2O_3 contents in pyrolite bulk mantle and in the basalt layer of subducted oceanic lithosphere range between 4 and 16 wt.% (Stolper, 1980; S. S. Sun, 1982). Thus, experiments in the MgO-Al_2O_3-SiO_2-H_2O (MASH) system and their results will reflect a more realistic picture of the phase relations in the Deep Earth. The incorporation of Al in the structure of DHMSs will expand their thermodynamic stabilities to higher P-T conditions (Kakizawa et al., 2018; Pamato et al., 2015; Xu et al., 2021). A recent study shows that shy-B with ~30 wt.% Al_2O_3 could remain stable up to 24 GPa and 2300 K (Kakizawa et al., 2018). Ph-D with 21 wt.% Al_2O_3 is stable between 14 GPa, 1200 K and at least 25 GPa, 1800 K and the Al-end-member of Ph-D ($Al_2SiO_4(OH)_2$) has been proven to be stable at 26 GPa and 2300 K (Pamato et al., 2015; Xu et al., 2019). However, the dehydration boundaries and the decomposition products of Al-bearing shy-B and Ph-D at high P-T are still poorly constrained and need to be further explored. In this study, we investigated in-situ the thermal phase stability of Al-bearing shy-B and Ph-D up to 55 GPa and 2500 K. The dehydration boundaries and decomposition products of Al-bearing shy-B and Ph-D were determined at high P-T conditions. Our results add a piece to the puzzle that might clarify the water cycle in the topmost lower mantle.

2. Experiments

Al-free and Al-bearing shy-B (Al-shy B) were synthesized in a rotating multi-anvil press at the GFZ, Potsdam. The chemical compositions are $Mg_{9.39}Si_{2.93}Al_{0.04}H_{5.37}O_{18}$ and $Mg_{8.04}Si_{2.17}Al_{1.35}O_{18}H_{7.18}$, respectively. Details of the multi-anvil press setup, the synthesis and characterization of the shy-B are reported in Deon et al. (2011) and Li et al. (2022), respectively. Both resistive and laser heating experiments in diamond anvil cells (RH-DACs, LH-DACs) were performed in this study.

The RH-DAC experiments were performed using a four-pin DAC (4pDAC) equipped with an internal graphite heater (details for the setup can be found in Carl et al. (2018), Liermann et al. (2009)). The RH-DAC and a cooling holder made of copper were placed into a vacuum vessel to avoid the oxidation of components of the RH-DAC assembly. The XRD experiments were performed at the Extreme Conditions Beamline (ECB, P02.2) at PETRA III, DESY (Hamburg, Germany). X-ray diffraction (XRD) images were collected in steps of 100 K and 3–5 GPa up to 35 GPa and 1280 K. At each P-T point the sample was heated for about 1 hr. More details about sample loading and beamline setup can be found in Text 1 in Supporting Information S1.

In the laser heating experiments, a pellet of finely powdered shy-B (gently packed between two diamonds) was sandwiched between 2 pieces of 2 μm thick Pt foil. Several small grains of Al-bearing shy-B were placed on the two diamonds culets providing space for the pressure transmitting medium while preventing the direct contact between Pt foils and diamonds (Figure S1 in Supporting Information S1). Re gaskets were pre-indented to 30 μm in thickness and a 150 μm hole was drilled at the center of the indentation, acting as the sample chamber. Ne was loaded into the chamber as a thermal insulator and pressure transmitting medium. In the LH experiments, using a beamsplitter, one laser (λ = 1,072 nm) was split into two separate beams, each focused on one of the two sides of the sample in the DAC while the hot-spot produced by the two laser beams was aligned with the X-ray beam. XRD images were collected before, during and after each heating cycle with collection times of 20 s (see Supporting Information S1 for details).

3. Results and Discussions

3.1. Phase Stability of Al-Bearing Shy-B and Ph-D

The P-T conditions and results of RH-DAC experiments are shown in Table S1 and Figure S2 in Supporting Information S1. Due to the presence of pyrope coexisting with Al-bearing shy-B in the starting materials, the RH-experiments contained some pyrope. At each selected pressure-temperature point, the entire sample chamber was mapped by X-ray diffraction on a 7 × 7 grid (with a step size of 6 μm) by means of a 3 (v) × 8 (h) μm^2 X-ray beam to locate the best position with maximum signal from Al-bearing shy-B. Our results show that Al-bearing shy-B with 1.35 Al pfu remains stable without any decomposition up to 34.5(9) GPa and 1280 K (Table S1 and Figure S2 in Supporting Information S1). A previous study using the LVP shows that Al-free shy-B decomposed at 30 GPa and 900 K (Ohtani et al., 2003). This indicates that the incorporation of Al in the structure of shy-B expands its phase stability to higher temperature.

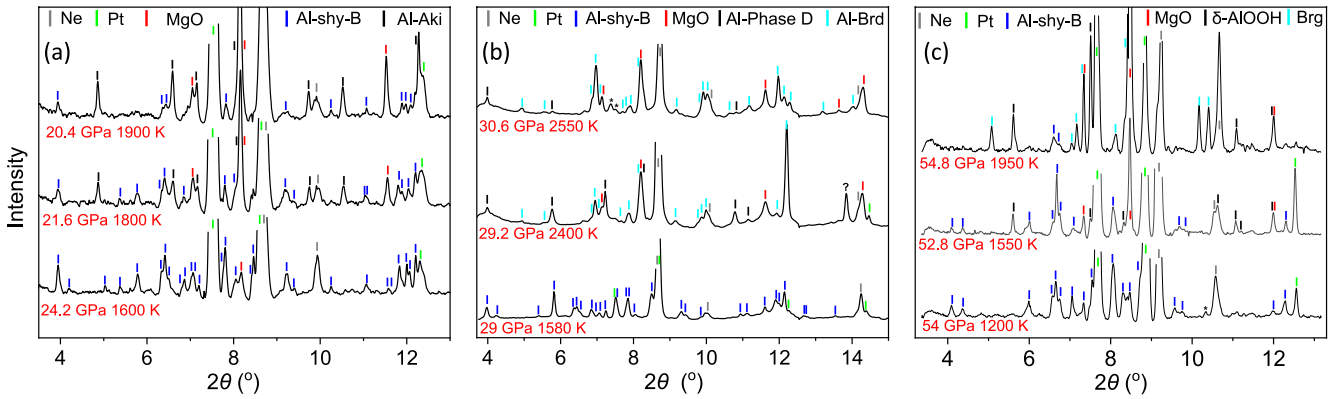

Figure 1. Representative X-ray diffraction patterns of Al-bearing shy-B at high pressures between 20 and 55 GPa and high temperatures between 1200 and 2550 K. Ne: neon; Pt: platinum; Al-shy-B: Al-bearing superyhydrous phase B; Al-Aki: Al-bearing akimotoite; Al-Phase D: Al-bearing phase D; Al-Brd: Al bearing bridgmanite; Brd: bridgmanite. The asterisks indicate peaks of Pt hydride (PtH_X); the question mark indicates an unknown peak. Note that: in (c), due to the very limited Al-bearing shy-B at 54.8 GPa and 1950 K, we consider that the Al-bearing shy-B should be metastable in this condition.

The phase stability of Al-bearing and Al-free shy-B were also investigated in LH-DACs. The experimental details are listed in Table S1 in Supporting Information S1. Pt was used as pressure marker up to the decomposition of shy-B. After shy-B decomposition, the release of H_2O caused a reaction with Pt forming PtH_X rendering Pt useless for pressure determination (Sano et al., 2008; Schwager et al., 2004). Therefore, MgO produced during the breakdown of shy-B was used as a pressure calibrant (Speziale et al., 2001). Our high P-T experiments show that Al-free shy-B decomposes to MgO and ringwoodite at 24 GPa and 1800 K (Table S1 in Supporting Information S1). Along the 30 GPa quasi-isobar, with increasing temperature, we first observe the decomposition of Al-free shy-B to Ph-D and MgO at 1800 K followed by the transition of Al-free Ph-D to bridgmanite at 2000 K (Table S1 in Supporting Information S1). We note that, in our LH-experiments on Al-free shy-B, the starting temperature of the dehydration experiment was 1800 K; thus, this data point only represents an upper bound of the dehydration reaction of Al-free shy-B, while the actual thermodynamic boundary is located at lower T, as indicated in Ohtani et al. (2003).

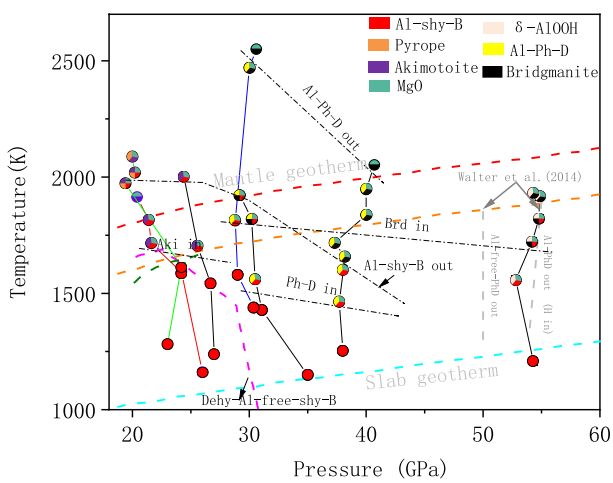

Figure 2. Reaction diagram of Al-bearing shy-B between 20 and 55 GPa at 1200–2500 K. Dashed red curve: average mantle geotherm; orange dashed curve: temperature profile of the interface between basalt and peridotite layer; cyan curve: thermal profile of a cold slab. The magenta dashed line represents the dehydration boundary of Al-free shy-B from Ohtani et al. (2003). The green dashed line indicates the dehydration of Al-bearing DHMSs from Xu et al. (2021). Dashed gray lines: stability limit of Al-free and Al-bearing phase D form Walter et al. (2015). The solid lines indicate the P-T experimental paths for each heating cycle (red, green and blue are used to distinguish two similar P-T paths, respectively). The dash dotted lines indicate the reaction boundary between different phases.

The decomposition products of Al-bearing shy-B strongly depend on the P-T path followed during the experiments. For example, heating at a starting pressure of 22 GPa resulted in the decomposition of Al-bearing shy-B to pyrope and akimotoite at 20 GPa and 2000 K. The formation of pyrope is most probably caused by a change of the P-T conditions from 24 GPa to 1600 K to 20 GPa and 2000 K during the heating; the pressure decrease could lower the Al content in akimotoite and promote the formation of pyrope (Kubo & Akaogi, 2000). At higher pressure conditions, two other experimental runs indicate that Al-bearing shy-B starts to transform to MgO and akimotoite without pyrope at 22–26 GPa above ~1600 K (Figures 1a and 2). With increasing temperature, Al-bearing shy-B completely transforms to akimotoite and MgO at ~2000 K (Figures 1a and 2). We also observed the phase transition from akimotoite to bridgmanite at 24 GPa and 2000 K (Table S1 in Supporting Information S1). However, the P-T conditions changed to 30 GPa and 1700 K after the phase transition. It is worth mentioning that this is the only P-T path which crossed the phase transition between akimotoite and bridgmanite in all our experiments. The result also indicates that the phase transition between akimotoite and bridgmanite in the presence of H_2O and Al is located at 24–30 GPa and 2000 K (corresponding to 660–800 km depth in Earth's mantle) that is at conditions of the topmost lower mantle. The results further suggest that Al-bearing akimotoite is not a low temperature phase but can remain stable up to 2000 K.

The experiments in the pressure range between 30 and 40 GPa show that Al-bearing shy-B starts to transform to Al-bearing Ph-D and MgO at 1600 and 1400 K (Figures 1b and 2); thereafter it coexists with Al-bearing Ph-D and MgO up to 1900 and 1670 K at 29 and 38 GPa, respectively (Figures 1b and 2). Bridgmanite is then formed at 1800 K, 29 GPa and at 1700 K, 37 GPa in the two experiments. Interestingly, our results indicate that Al-bearing Ph-D could coexist with bridgmanite and remain stable up to 2400 and 2000 K at 30 and 40 GPa (Figures 1b and 2). At higher pressure, Al-bearing shy-B transforms to MgO and δ-AlOOH phase at 52 GPa and 1430 K. With increasing temperature, bridgmanite forms at 54.8 GPa and 1700 K and Al-bearing shy-B completely decomposes at 1900 K (Figure 1c).

Our results place first constraints on the dehydration boundary and the decomposition products for Al-bearing shy-B in the pressure range between 20 and 54.8 GPa. The phase stability of Al-free shy B has been fully investigated by in situ X-ray diffraction experiments in a LVP (Ohtani et al., 2003). Al-free shy-B decomposes to MgO, hydrous ringwoodite, Ph-D, bridgmanite and H_2O, and the decomposition boundary shows a negative Clapeyron slope (Ohtani et al., 2003) as it is also shown in Figure 2. Our result suggests that the incorporation of Al in the system will significantly change the phase relations in the DHMSs. Between 20 and 24 GPa, the incorporation of Al could inhibit the formation of hydrous ringwoodite and promote the formation of akimotoite and MgO. However, a recent study using the LVP did not observe the formation of Al-bearing akimotoite in the same pressure range (Xu et al., 2019). The incorporation of Al will also expand the stability of shy-B to higher temperatures between 20 and 24 GPa. Al-free shy-B transforms to MgO, Ph-D and bridgmanite at ∼1000 K and 30 GPa (Ohtani et al., 2003). However, both our RH- and LH-experiments show that Al-bearing shy-B is preserved at temperatures up to ∼600 K higher temperature than the Al-free composition at 30 GPa. A previous study on shy-B with 7–14 wt.% Al_2O_3 shows that it could remain stable to 24 GPa and 1700–1900 K (Kakizawa et al., 2018), which is 100 K lower, however compatible within uncertainties with the dehydration boundary determined in our study, that is 2000 ± 200 K. Such agreement also confirms our claim that our experiments probe equilibrium conditions.

The phase stability of Al-bearing Ph-D may also be assessed using the data from this study. Previous studies of the MSH system show that Ph-D is stable at 30–50 GPa and 1200–1800 K (Walter et al., 2015). In contrast, when Al_2O_3 is added to the system, the experiments on the MASH system indicate that Ph-D could coexist with bridgmanite and phase H between 35 and 54 GPa at 1400–1800 K (Walter et al., 2015). Our results show that Al-bearing Ph-D can remain stable at 28 GPa and 1800 K and it is not stable at pressures beyond 53 GPa, which is consistent with previous studies (Walter et al., 2015). According to the results of Pamato et al. (2015) and Xu et al. (2019), Al-bearing Ph-D could remain stable up to 26 GPa and 2300 K but the decomposition boundary was still unknown until now. Another study shows that 1 wt.% Al_2O_3 in the MASH system could increase the stability of Ph-D by ∼200 K and delay its decomposition to 2000 K and 24 GPa (Ghosh & Schmidt, 2014). Our results with higher Al content in the system indicate that Al-bearing Ph-D could remain stable up to 2400 K at 30 GPa which is much higher than the reported stability limit for Al-free Ph-D determined in previous studies (e.g., Nishi et al., 2014).

3.2. Al Partition in the Mantle Minerals at High Pressure and Temperature

The experiments we performed also provide information about the partitioning of Al in the phases produced by the breakdown of Shy-B, that is akimotoite, bridgmanite and δ-AlOOH in the different pressure regimes. Using the XRD measurements performed at high pressure after temperature quenching, we determined the unit-cell parameters of the decomposition products, akimotoite and bridgmanite, at high pressures and 300 K (Figure 3). The unit-cell volume of akimotoite, formed during decomposition of Al-bearing shy-B, is 1.6% smaller than that of Al-free akimotoite (Wang et al., 2004). Both theoretical and experimental studies indicate that the incorporation of Al in the structure of akimotoite produces a decrease of its unit-cell volume (Panero et al., 2006; Siersch, 2019). The unit-cell volume of akimotoite in our experiment is also smaller compared to the unit-cell volume of akimotoite with 20 mol % Al_2O_3 (Siersch, 2019) (Figure 3a). Our interpretation is that the Al content in our akimotoite is higher than 20 mol%: if during the decomposition of Al-bearing shy-B all the Al released from shy-B dissolves in the structure of akimotoite, the Al_2O_3 content in akimotoite would be 23.8 mol% with a $(Mg_{0.763}Al_{0.238})$ $(Al_{0.238}Si_{0.763})O_3$ composition. Thus, the small unit-cell volume of akimotoite in this study indicates that indeed all Al_2O_3 from Al-bearing shy-B was incorporated into akimotoite. This interpretation is further

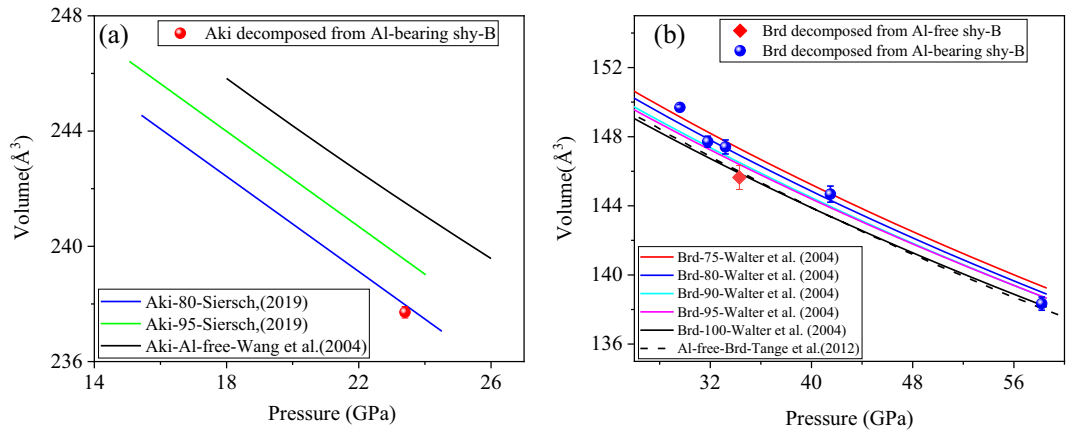

Figure 3. Comparison of the unit-cell volumes of akimotoite and bridgmanite with different Al-content at high pressure and 300 K. (a) Compression curves of akimotoite with different Al contents; akimotoite in our experiment is produced by the decomposition of Al-bearing shy-B. Blue line: Al-free akimotoite (Wang et al., 2004); green line: 5 mol.% Al-bearing akimotoite (Siersch, 2019); black line: 20 mol.% Al-bearing akimotoite (Siersch, 2019). (b) Compression curves of bridgmanite with different Al contents. Bridgmanite observed in our experiments is a decomposition product of Al-bearing and Al-free shy-B. The dashed line represents the results of Al-free bridgmanite from Tange et al. (2012). Red, blue, cyan, magenta lines indicate the unit-cell volumes of bridgmanite with 25, 20, 10, 5, and 0 mol.% Al-content (Walter et al., 2004).

supported by the fact that our XRD images do not show peaks belonging to any independent Al_2O_3 phase such as corundum (Figure 1a).

The unit-cell volume of bridgmanite produced by the decomposition of Al-free and Al-bearing shy-B was also determined at high pressure and 300 K, that is, after temperature quenching (Figure 3). Previous studies indicate that Al incorporation increases the unit-cell volume of bridgmanite (Liu, Irifune, Nishi, et al., 2016; Liu, et al., 2017; Panero et al., 2006; Walter et al., 2004). Thus, the unit-cell volume could be used to infer the Al content in bridgmanite. Our results show that the unit-cell volume of bridgmanite, formed during the decomposition of Al-free shy-B, is equal to that of Al-free bridgmanite (Figure 3b). In contrast, the bridgmanite formed between 30 and 40 GPa during the decomposition of Al-bearing shy-B has a much larger unit-cell volume than the Al-free composition suggesting that in these experiments Al is incorporated into the structure of bridgmanite. We compared the unit-cell volumes determined in this study with those of bridgmanite with 0–25 mol.% Al_2O_3 content (Tange et al., 2012; Walter et al., 2004). However, the equation of state (EoS) of Al-free bridgmanite by Tange et al. (2012) is different from that obtained by Walter et al. (2004) and the difference is most probably caused by the systematic disagreement between the pressure scales used in these studies. MgO was used as the pressure calibrant in our study and in the work by Tange et al. (2012), while KBr was used as the pressure calibrant in Walter et al. (2004). Although there is a difference between the MgO pressure scales of Speziale et al. (2001), the one we use to determine pressure in our experiments, and that of Tange et al. (2009) at high temperature, the difference is less than 1 GPa at 300 K. To compare the results of the different studies, we corrected the pressures in Walter et al. (2004) to MgO (details can be found in in Supporting Information S1) using the results by Tange et al. (2012) as a reference. The comparison of the unit-cell volumes of bridgmanite reveals that the decomposition product of Al-bearing shy-B in our experiments has an Al_2O_3 content ~20–25 mol % which is consistent with the estimation from the reaction. The significantly increased unit-cell volume of bridgmanite indicates that all the Al_2O_3 decomposed from Al-bearing shy-B could be incorporated into the structure of bridgmanite between 28 and 42 GPa. More interestingly, bridgmanite produced by our heating experiment at 52–54.8 GPa, and T-quenched (Figure 3b; in this case pressure increases to 58 GPa due to temperature quenching) has a unit-cell volume equal to that of Al-free bridgmanite. This indicates that the Al content in bridgmanite in this study is very small at pressures above 52 GPa. The reduced Al content in bridgmanite at these conditions can be explained with high Al partitioning into δ-AlOOH rather than into coexisting bridgmanite. Similar to our results, Ohira et al. (2014) showed that Al-bearing bridgmanite could react with water forming the solid solution of δ-AlOOH—$MgSiO_2(OH)_2$ and preventing Al incorporation in bridgmanite between 68 GPa and 2010 K. Our study, however, indicates that the Al-depleted bridgmanite can be formed already between 52 and 54.8 GPa. In addition, a recent study also indicates strong Al partitioning in both Ph-D and Phase H resulting in Al-depleted

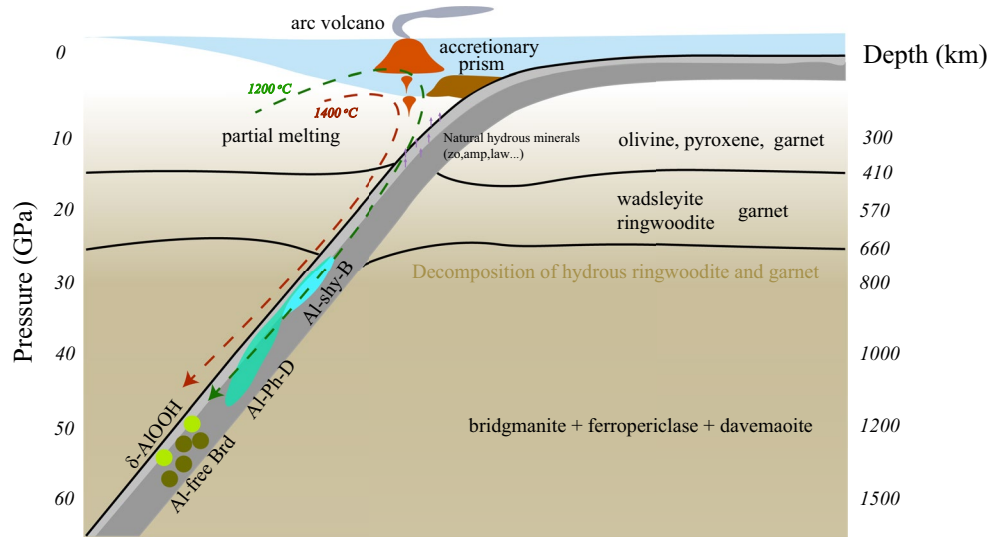

Figure 4. Schematic mantle cross-section describing H_2O transport via Al-bearing dense hydrous magnesium silicates (DHMSs) in subducted oceanic lithosphere slabs. Zo: zoesite; amp: amphibole; law: lawsonite. The other abbreviations are the same as in Figure 2.

bridgmanite between 25 and 28 GPa and 1300–1400 K (Ishii et al., 2022). Due to dehydration of Al-bearing Ph-D at high temperature, we did not observe the coexistence of bridgmanite and Ph-D in the quenched sample in our study. Consequently, we could not determine the Al partitioning between the Ph-D and bridgmanite at relatively low temperatures. Because of the technical challenges involved in recovering the DAC samples after the experiment and its high failure rate, we were not able at this time to match the in situ XRD partitioning estimations with electron microprobe analysis (EMPA) of the recovered samples. A dedicated partitioning study could be part of future work. In conclusion, our observations support the hypothesis that in the Al-bearing MASH system, Al preferentially partitions in δ-AlOOH rather than in bridgmanite at pressures between 52 and 54.8 GPa.

4. Geophysical Implications

Shy-B and Ph-D are important water carriers into the deep Earth's interior. Their thermal stability is crucial for understanding the transport of water in the mantle transition zone and lower mantle (Frost & Fei, 1998; Ohtani, 2005). Al_2O_3 content is equal to 4 wt.% in the pyrolite mantle and 16 wt.% in the basaltic crust layer of subducted oceanic lithosphere (Stolper, 1980; S. S. Sun, 1982). In the upper mantle Al is mostly incorporated in garnet which transforms to bridgmanite and Ca-perovskite (davemaoite) at the bottom of the transition zone (Irifune & Tsuchiya, 2015). Studies on the MORB-H_2O system show that no hydrous phases can be formed at depths below ~300 km (Ohtani, 2005; Okamoto & Maruyama, 2004). Hydrous ringwoodite and garnet decompose in the subducted slabs at topmost lower mantle depths, providing Al and water rich conditions. Liu et al. (2017) showed that the solubility of Al_2O_3 in bridgmanite is 6.7 mol% (6.8 wt.%) at 27 GPa and 1700 K. Thus, a large fraction of the Al content of the basalt layer cannot be incorporated into the bridgmanite and the excess Al may drive the formation of Al-bearing shy-B. In addition, the Al partition coefficient between shy-B and bridgmanite increases with temperature (Kakizawa et al., 2018). We thus conclude that deeply subducted oceanic slabs reaching depths of the topmost lower mantle, being relatively colder than the surrounding mantle, are favorable environments for the formation of Al-bearing shy-B at the interface (transition) between the basaltic crust and the underlying subducted peridotite layer (IBPL). Our new high-pressure-temperature reaction diagram for Al-bearing shy-B can help to describe the water transport in the subducting slabs. As the upper layer of the subducted slab is heated by the overlaying bulk mantle, we can assume that the temperature of the IBPL is 200 K lower than the bulk overlaying mantle (Syracuse et al., 2010). In this scenario (Figure 4), Al-bearing shy-B could transport H_2O to the depth of ~1,000 km and then decompose to Al-bearing Ph-D and Al-depleted bridgmanite. At depths larger than 1,000 km Al-bearing Ph-D is the main hydrous phase coexisting with Al-bearing bridgmanite. Along the IBPL thermal profile which is 200 K lower than the average mantle geotherm, most of Al-bearing Ph-D decomposes and releases H_2O to the mantle at the depth of 1,300 km.

Below 1,300 km depth δ-AlOOH should be the major phase transporting H_2O to the core-mantle boundary. Our results also indicate that Al partitions into δ-AlOOH rather than into bridgmanite at 55 GPa and 1900 K. Previous studies also indicate that H_2O could react with Al-bearing bridgmanite producing δ-AlOOH, phase H ($MgSiO_2(OH)_2$) and Al-poor bridgmanite (Ohira et al., 2014). Using the unit-cell volume of bridgmanite as a constraint, our results indicate that the chemical composition of bridgmanite coexisting with δ-AlOOH is close to Al-free. Although studies on the phase stability of δ-AlOOH are still controversial, they all conclude that δ-AlOOH could be the carrier of H_2O deep down to the lowermost mantle which would extend the cycle of H_2O in the Earth interior down to 2,100 km or even to the core-mantle boundary at ∼2,900 km (Duan et al., 2018; Piet et al., 2020). Some recent studies indicate that the phase transition of Fe- and Al-depleted bridgmanite to post-perovskite could explain the observed complex seismic structures in D'' beneath North and Central America (van der Hilst et al., 2007; Kawai, Geller, et al., 2007; Kawai, Takeuchi, et al., 2007; N. Sun et al., 2018). Our results suggest that the presence of DHMS phases in subducted slabs even at mid-lower mantle depth could also control the Al content of bridgmanite producing Al-depleted bridgmanite ultimately affecting the seismic signature of the D'' discontinuity.

It should however be noted that Fe is a critical element in the interpretation of the structure and properties of the Earth's mantle. Fe can be incorporated into the structure of DHMSs (e.g., Crichton et al., 1999; Ghosh & Schmidt, 2014; Shieh et al., 1998). In the absence of systematic experimental data on the effect of Fe on the stability of Al-bearing DHMSs, one previous study indicates that the incorporation of Fe and that of Al have opposite effects on the stability of Ph-D at 24 GPa (Ghosh & Schmidt, 2014).

Ghosh and Schmidt (2014) show that the addition of 1 wt.% Al_2O_3 in the structure of Ph-D could expands its thermal stability by 200 K, while the combined incorporation of 1 wt% Al_2O_3 and 4.3 wt.% FeO does not modify the thermal stability of Ph-D with respect to the Al-free Mg-endmember. Based on this we suggest that the effect of 1 wt.% Al_2O_3 on the phase stability of Ph-D could be balanced by that of 4.3 wt.% FeO (Ghosh & Schmidt, 2014). However, in a realistic scenario similar to our IBPL model, the basaltic layer contains 4–16 wt.% Al_2O_3 and ∼10 wt.% FeO which is very different from the compositions considered by Ghosh and Schmidt (2014). In the absence of a systematic knowledge of the relative partitioning of Al and Fe in shy-B and other DHMS phases, we are unable to quantify their combined effect on the stability of shy-B and Ph-D in deeply subducted oceanic plates.

While our study of the reaction behavior and phase stability of shy-B and Ph-D only considers the Fe-free system, one may argue that in Al-rich systems like in IBPL more Al is probably incorporated in DHMSs than in the relatively Al-poor, Fe-bearing systems (like the only examined by Ghosh & Schmidt, 2014) and consequently the effect of Al incorporation rather than that of Fe controls the phase stability of DHMSs. However, the incorporation of any amount of Fe would significantly increase the density of DHMSs with additional consequences on the thermodynamic and seismic properties of these phases, further complicating the scenario. Thorough investigations of the stability and thermal equation of state of (Fe, Al)-bearing DHMSs are needed.

Data Availability Statement

All the data for the phase diagram and unit-cell parameters are available on Zenodo (https://doi.org/10.5281/zenodo.6320835).

Acknowledgments
We are grateful to the two anonymous reviewers whose comments have greatly improved the quality of the manuscript. We acknowledge the scientific exchange and support of the Center for Molecular Water Science (CMWS) as part of the early science program (DESY and GFZ). We also acknowledge DESY (Hamburg, Germany), a member of the Helmholtz Association HGF, for the provision of the experimental facilities. The experiments were carried out at beamline P02.2 and used facilities provided by the Extreme Condition Science Infrastructure (ECSI) of PETRA III. Open Access funding enabled and organized by Projekt DEAL.

References

Brudzinski, M. R., & Chen, W.-P. (2003). A petrologic anomaly accompanying outboard earthquakes beneath Fiji-Tonga: Corresponding evidence from broadband *P* and *S* waveforms: Mantle structure, seismicity and petrology. *Journal of Geophysical Research*, *108*(B6), 2229. https://doi.org/10.1029/2002JB002012

Carl, E.-R., Liermann, H.-P., Ehm, L., Danilewsky, A., & Kenkmann, T. (2018). Phase transitions of α-quartz at elevated temperatures under dynamic compression using a membrane-driven diamond anvil cell: Clues to impact cratering? *Meteoritics & Planetary Science*, *53*(8), 1687–1695. https://doi.org/10.1111/maps.13077

Crichton, W. A., Ross, N. L., & Gasparik, T. (1999). Equations of state of magnesium silicates anhydrous B and superhydrous B. *Physics and Chemistry of Minerals*, *26*(7), 570–575. https://doi.org/10.1007/s002690050220

Deon, F., Koch-Müller, M., Rhede, D., & Wirth, R. (2011). Water and Iron effect on the P-T-x coordinates of the 410-km discontinuity in the Earth upper mantle. *Contributions to Mineralogy and Petrology*, *161*(4), 653–666. https://doi.org/10.1007/s00410-010-0555-6

Di Leo, J. F., Wookey, J., Hammond, J. O. S., Kendall, J.-M., Kaneshima, S., Inoue, H., et al. (2012). Deformation and mantle flow beneath the Sangihe subduction zone from seismic anisotropy. *Physics of the Earth and Planetary Interiors*, *194–195*, 38–54. https://doi.org/10.1016/j.pepi.2012.01.008

Duan, Y., Sun, N., Wang, S., Li, X., Guo, X., Ni, H., et al. (2018). Phase stability and thermal equation of state of δ-AlOOH: Implication for water transportation to the deep lower mantle. *Earth and Planetary Science Letters*, *494*, 92–98. https://doi.org/10.1016/j.epsl.2018.05.003

Frost, D. (1999). The stability of dense hydrous magnesium silicates in Earth's transition zone and lower mantle. *Mantle Petrology, Special Publication No.*, *6*, 14.

Frost, D. J., & Fei, Y. (1998). Stability of phase D at high pressure and high temperature. *Journal of Geophysical Research*, *103*(B4), 7463–7474. https://doi.org/10.1029/98JB00077

Ghosh, S., & Schmidt, M. W. (2014). Melting of phase D in the lower mantle and implications for recycling and storage of H_2O in the deep mantle. *Geochimica et Cosmochimica Acta*, *145*, 72–88. https://doi.org/10.1016/j.gca.2014.06.025

Irifune, T., & Tsuchiya, T. (2015). Phase transitions and mineralogy of the lower mantle. In *Treatise on Geophysics* (pp. 33–60). Elsevier. https://doi.org/10.1016/B978-0-444-53802-4.00030-0

Ishii, T., Ohtani, E., & Shatskiy, A. (2022). Aluminum and hydrogen partitioning between bridgmanite and high-pressure hydrous phases: Implications for water storage in the lower mantle. *Earth and Planetary Science Letters*, *8*, 117441. https://doi.org/10.1016/j.epsl.2022.117441

Kakizawa, S., Inoue, T., Nakano, H., Kuroda, M., Sakamoto, N., & Yurimoto, H. (2018). Stability of Al-bearing superhydrous phase B at the mantle transition zone and the uppermost lower mantle. *American Mineralogist*, *103*(8), 1221–1227. https://doi.org/10.2138/am-2018-6499

Kawai, K., Geller, R. J., & Fuji, N. (2007). D″ beneath the Arctic from inversion of shear waveforms. *Geophysical Research Letters*, *34*(21), L21305. https://doi.org/10.1029/2007GL031517

Kawai, K., Takeuchi, N., Geller, R. J., & Fuji, N. (2007). Possible evidence for a double crossing phase transition in D″ beneath Central America from inversion of seismic waveforms: Possible double crossing in D. *Geophysical Research Letters*, *34*(9). https://doi.org/10.1029/2007GL029642

Koch-Müller, M., Dera, P., Fei, Y., Hellwig, H., Liu, Z., Orman, J. V., & Wirth, R. (2005). Polymorphic phase transition in superhydrous phase B. *Physics and Chemistry of Minerals*, *32*(5–6), 349–361. https://doi.org/10.1007/s00269-005-0007-4

Kubo, A., & Akaogi, M. (2000). Post-garnet transitions in the system $Mg_4Si_4O_{12}$–$Mg_3Al_2Si_3O_{12}$ up to 28 GPa: Phase relations of garnet, ilmenite and perovskite. *Physics of the Earth and Planetary Interiors*, *121*(1–2), 85–102. https://doi.org/10.1016/S0031-9201(00)00162-X

Li, X., Mao, Z., Sun, N., Liao, Y., Zhai, S., Wang, Y., et al. (2016). Elasticity of single-crystal superhydrous phase B at simultaneous high pressure-temperature conditions: Elasticity of Shy-B. *Geophysical Research Letters*, *43*(16), 8458–8465. https://doi.org/10.1002/2016GL070027

Li, X., Speziale, S., Glazyrin, K., Wilke, F. D. H., Liermann, H.-P., & Koch-Müller, M. (2022). Synthesis, structure, and single-crystal elasticity of Al-bearing superhydrous phase B. *American Mineralogist*, *107*(5), 885–895. https://doi.org/10.2138/am-2022-7989

Liermann, H.-P., Merkel, S., Miyagi, L., Wenk, H.-R., Shen, G., Cynn, H., & Evans, W. J. (2009). Experimental method for *in situ* determination of material textures at simultaneous high pressure and high temperature by means of radial diffraction in the diamond anvil cell. *Review of Scientific Instruments*, *80*(10), 104501. https://doi.org/10.1063/1.3236365

Liu, Z., Irifune, T., Nishi, M., Tange, Y., Arimoto, T., & Shinmei, T. (2016). Phase relations in the system $MgSiO_3$–Al_2O_3 up to 52 GPa and 2000 K. *Physics of the Earth and Planetary Interiors*, *257*, 18–27. https://doi.org/10.1016/j.pepi.2016.05.006

Liu, Z., Nishi, M., Ishii, T., Fei, H., Miyajima, N., Ballaran, T. B., et al. (2017). Phase relations in the system $MgSiO_3$-Al_2O_3 up to 2300 K at lower mantle pressures: Phase relations and Al in bridgmanite. *Journal of Geophysical Research: Solid Earth*, *122*(10), 7775–7788. https://doi.org/10.1002/2017JB014579

Liu, Z., Park, J., & Karato, S. (2016). Seismological detection of low-velocity anomalies surrounding the mantle transition zone in Japan subduction zone. *Geophysical Research Letters*, *43*(6), 2480–2487. https://doi.org/10.1002/2015GL067097

Nishi, M., Irifune, T., Tsuchiya, J., Tange, Y., Nishihara, Y., Fujino, K., & Higo, Y. (2014). Stability of hydrous silicate at high pressures and water transport to the deep lower mantle. *Nature Geoscience*, *7*(3), 224–227. https://doi.org/10.1038/ngeo2074

Ohira, I., Ohtani, E., Sakai, T., Miyahara, M., Hirao, N., Ohishi, Y., & Nishijima, M. (2014). Stability of a hydrous δ-phase, AlOOH–$MgSiO_2(OH)_2$, and a mechanism for water transport into the base of lower mantle. *Earth and Planetary Science Letters*, *401*, 12–17. https://doi.org/10.1016/j.epsl.2014.05.059

Ohtani, E. (2005). Water in the mantle. *Elements*, *1*(1), 25–30. https://doi.org/10.2113/gselements.1.1.25

Ohtani, E. (2020). The role of water in Earth's mantle. *National Science Review*, *7*(1), 224–232. https://doi.org/10.1093/nsr/nwz071

Ohtani, E., Toma, M., Kubo, T., Kondo, T., & Kikegawa, T. (2003). In situ X-ray observation of decomposition of superhydrous phase B at high pressure and temperature. *Geophysical Research Letters*, *30*(2), 1029. https://doi.org/10.1029/2002GL015549

Okamoto, K., & Maruyama, S. (2004). The Eclogite–Garnetite transformation in the MORB+H_2O system. *Physics of the Earth and Planetary Interiors*, *146*(1–2), 283–296. https://doi.org/10.1016/j.pepi.2003.07.029

Palot, M., Jacobsen, S. D., Townsend, J. P., Nestola, F., Marquardt, K., Miyajima, N., et al. (2016). Evidence for H_2O-bearing fluids in the lower mantle from diamond inclusion. *Lithos*, *265*, 237–243. https://doi.org/10.1016/j.lithos.2016.06.023

Pamato, M. G., Myhill, R., Boffa Ballaran, T., Frost, D. J., Heidelbach, F., & Miyajima, N. (2015). Lower-mantle water reservoir implied by the extreme stability of a hydrous aluminosilicate. *Nature Geoscience*, *8*(1), 75–79. https://doi.org/10.1038/ngeo2306

Panero, W. R., Akber-Knutson, S., & Stixrude, L. (2006). Al_2O_3 incorporation in $MgSiO_3$ perovskite and ilmenite. *Earth and Planetary Science Letters*, *252*(1–2), 152–161. https://doi.org/10.1016/j.epsl.2006.09.036

Pearson, D. G., Brenker, F. E., Nestola, F., McNeill, J., Nasdala, L., Hutchison, M. T., et al. (2014). Hydrous mantle transition zone indicated by ringwoodite included within diamond. *Nature*, *507*(7491), 221–224. https://doi.org/10.1038/nature13080

Piet, H., Leinenweber, K. D., Tappan, J., Greenberg, E., Prakapenka, V. B., Buseck, P. R., & Shim, S.-H. (2020). Dehydration of δ-AlOOH in earth's deep lower mantle. *Minerals*, *10*(4), 384. https://doi.org/10.3390/min10040384

Rosa, A. D., Sanchez-Valle, C., Nisr, C., Evans, S. R., Debord, R., & Merkel, S. (2013). Shear wave anisotropy in textured phase D and constraints on deep water recycling in subduction zones. *Earth and Planetary Science Letters*, *377*(378), 13–22. https://doi.org/10.1016/j.epsl.2013.06.036

Rosa, A. D., Sanchez-Valle, C., Wang, J., & Saikia, A. (2015). Elasticity of superhydrous phase B, seismic anomalies in cold slabs and implications for deep water transport. *Physics of the Earth and Planetary Interiors*, *243*, 30–43. https://doi.org/10.1016/j.pepi.2015.03.009

Sano, A., Ohtani, E., Kondo, T., Hirao, N., Sakai, T., Sata, N., et al. (2008). Aluminous hydrous mineral δ-AlOOH as a carrier of hydrogen into the core-mantle boundary. *Geophysical Research Letters*, *35*(3), L03303. https://doi.org/10.1029/2007GL031718

Schmandt, B., Jacobsen, S. D., Becker, T. W., Liu, Z., & Dueker, K. G. (2014). Dehydration melting at the top of the lower mantle. *Science*, *344*(6189), 1265–1268. https://doi.org/10.1126/science.1253358

Schwager, B., Chudinovskikh, L., Gavriliuk, A., & Boehler, R. (2004). Melting curve of H_2O to 90 GPa measured in a laser-heated diamond cell. *Journal of Physics: Condensed Matter*, *16*(14), S1177–S1179. https://doi.org/10.1088/0953-8984/16/14/028

Shieh, S. R., Mao, H., Hemley, R. J., & Ming, L. C. (1998). Decomposition of phase D in the lower mantle and the fate of dense hydrous silicates in subducting slabs. *Earth and Planetary Science Letters*, *159*(1–2), 13–23. https://doi.org/10.1016/S0012-821X(98)00062-4

Siersch, N. C. (2019). The effect of Fe and Al on the elasticity of akimotoite (p. 195).

Speziale, S., Zha, C.-S., Duffy, T. S., Hemley, R. J., & Mao, H. (2001). Quasi-hydrostatic compression of magnesium oxide to 52 GPa: Implications fo`r the pressure-volume-temperature equation of state. *Journal of Geophysical Research*, *106*(B1), 515–528. https://doi.org/10.1029/2000JB900318

Stolper, E. (1980). A phase diagram for mid-ocean ridge basalts: Preliminary results and implications for petrogenesis. *Contributions to Mineralogy and Petrology*, *74*(1), 13–27. https://doi.org/10.1007/BF00375485

Sun, N., Wei, W., Han, S., Song, J., Li, X., Duan, Y., et al. (2018). Phase transition and thermal equations of state of (Fe, Al)-bridgmanite and post-perovskite: Implication for the chemical heterogeneity at the lowermost mantle. *Earth and Planetary Science Letters*, *490*, 161–169. https://doi.org/10.1016/j.epsl.2018.03.004

Sun, S.-S. (1982). Chemical composition and origin of the Earth's primitive mantle. *Geochimica et Cosmochimica Acta*, *46*(2), 179–192. https://doi.org/10.1016/0016-7037(82)90245-9

Syracuse, E. M., van Keken, P. E., & Abers, G. A. (2010). The global range of subduction zone thermal models. *Physics of the Earth and Planetary Interiors*, *183*(1–2), 73–90. https://doi.org/10.1016/j.pepi.2010.02.004

Tange, Y., Kuwayama, Y., Irifune, T., Funakoshi, K., & Ohishi, Y. (2012). *P-V-T* equation of state of $MgSiO_3$ perovskite based on the MgO pressure scale: A comprehensive reference for mineralogy of the lower mantle: *P-V-T* EOS OF $MgSiO_3$. *Journal of Geophysical Research*, *117*(B6). 6201. https://doi.org/10.1029/2011jb008988

Tange, Y., Nishihara, Y., & Tsuchiya, T. (2009). Unified analyses for *P-V-T* equation of state of MgO: A solution for pressure-scale problems in high *P-T* experiments. *Journal of Geophysical Research*, *114*(B3), B03208. https://doi.org/10.1029/2008JB005813

Tschauner, O., Huang, S., Greenberg, E., Prakapenka, V. B., Ma, C., Rossman, G. R., et al. (2018). Ice-VII inclusions in diamonds: Evidence for aqueous fluid in Earth's deep mantle. *Science*, *359*(6380), 1136–1139. https://doi.org/10.1126/science.aao3030

van der Hilst, R. D., de Hoop, M. V., Wang, P., Shim, S.-H., Ma, P., & Tenorio, L. (2007). Seismostratigraphy and thermal structure of Earth's core-mantle boundary region. *Science*, *315*(5820), 1813–1817. https://doi.org/10.1126/science.1137867

Walter, M. J., Kubo, A., Yoshino, T., Brodholt, J., Koga, K. T., & Ohishi, Y. (2004). Phase relations and equation-of-state of aluminous Mg-silicate perovskite and implications for Earth's lower mantle. *Earth and Planetary Science Letters*, *222*(2), 501–516. https://doi.org/10.1016/j.epsl.2004.03.014

Walter, M. J., Thomson, A. R., Wang, W., Lord, O. T., Ross, J., McMahon, S. C., et al. (2015). The stability of hydrous silicates in Earth's lower mantle: Experimental constraints from the systems $MgO–SiO_2–H_2O$ and $MgO–Al_2O_3–SiO_2–H_2O$. *Chemical Geology*, *418*, 16–29. https://doi.org/10.1016/j.chemgeo.2015.05.001

Wang, Y., Uchida, T., Zhang, J., Rivers, M. L., & Sutton, S. R. (2004). Thermal equation of state of akimotoite $MgSiO_3$ and effects of the akimotoite–garnet transformation on seismic structure near the 660 km discontinuity. *Physics of the Earth and Planetary Interiors*, *143–144*, 57–80. https://doi.org/10.1016/j.pepi.2003.08.007

Wookey, J., Kendall, J.-M., & Barruol, G. (2002). Mid-mantle deformation inferred from seismic anisotropy. *Nature*, *415*(6873), 777–780. https://doi.org/10.1038/415777a

Xu, C., Inoue, T., Kakizawa, S., Noda, M., & Gao, J. (2021). Effect of Al on the stability of dense hydrous magnesium silicate phases to the uppermost lower mantle: Implications for water transportation into the deep mantle. *Physics and Chemistry of Minerals*, *48*(9), 31. https://doi.org/10.1007/s00269-021-01156-4

Xu, C., Nishi, M., & Inoue, T. (2019). Solubility behavior of δ-AlOOH and ε-FeOOH at high pressures. *American Mineralogist*, *104*(10), 1416–1420. https://doi.org/10.2138/am-2019-7064

Yang, D., Wang, W., & Wu, Z. (2017). Elasticity of superhydrous phase B at the mantle temperatures and pressures: Implications for 800 km discontinuity and water flow into the lower mantle: High PT Elasticity of Superhydrous Phase. *Journal of Geophysical Research: Solid Earth*, *122*(7), 5026–5037. https://doi.org/10.1002/2017JB014319

References From the Supporting Information

Konôpková, Z., Morgenroth, W., Husband, R., Giordano, N., Pakhomova, A., Gutowski, O., et al. (2021). Laser heating system at the extreme conditions beamline, P02.2, PETRA III. *Journal of Synchrotron Radiation*, *28*(6), 1747–1757. https://doi.org/10.1107/S1600577521009231

Prescher, C., & Prakapenka, V. B. (2015). DIOPTAS: A program for reduction of two-dimensional X-ray diffraction data and data exploration. *High Pressure Research*, *35*(3), 223–230. https://doi.org/10.1080/08957959.2015.1059835